Journal of Alloys and Compounds 591 (2014) 85–90

Contents lists available at ScienceDirect

Journal of Alloys and Compounds

journal homepage: www.elsevier.com/locate/jalcom

Texture investigation of the superelastic Ti–24Nb–4Zr–8Sn alloy

Y. Yang [a], P. Castany [a,*], M. Cornen [a], I. Thibon [a], F. Prima [b], T. Gloriant [a]

[a] INSA Rennes, UMR CNRS 6226 ISCR, Laboratoire Chimie-Métallurgie, 20 Avenue des Buttes de Coësmes, 35708 Rennes, France
[b] Laboratoire de Physico-Chimie des Surfaces, Groupe de Métallurgie Structurale (UMR 7045), Chimie-ParisTech, Paris, France

ARTICLE INFO

Article history:
Received 20 December 2013
Accepted 23 December 2013
Available online 2 January 2014

Keywords:
Texture
Superelasticity
Titanium alloy
Tensile tests

ABSTRACT

In this work, the influence of crystallographic texture on mechanical properties was investigated by X-ray diffraction in the superelastic Ti–24Nb–4Zr–8Sn alloy. Different textures were obtained by changing the cold rolling reduction rate and the following thermal treatment (solution treatment or flash thermal treatment). The tensile tests performed show that Young's modulus, elongation at rupture and ultimate tensile strength are not influenced by texture. However, the superelastic property of the Ti–24Nb–4Zr–8Sn alloy after solution treatment clearly increases with the textural change into the γ-fiber texture with a $(1\,1\,1)[1\,\bar{2}\,1]$ main component due to the increase of cold rolling rate. Contrarily, the texture change induced by the increase of cold rolling rate has no influence on superelasticity after flash thermal treatment. Flash thermal treatment gives also higher recovery strain than solution treatment due to a smaller grain size.

1. Introduction

The Ti–24Nb–4Zr–8Sn alloy (Ti2448 for short later in this paper) is a new β-type multifunctional alloy (body-centered cubic structure). This alloy displays interesting properties such as high strength, low elastic modulus, high ductility, superelastic property and good biocompatibility. In previous works, different kinds of thermo-mechanical treatments were used for the processing of the alloy (cold deformation, hot rolling and warm rolling) [1–6]. Thanks to these investigations, a superelasticity of about 3.3% was obtained [3–6], which is much higher than the values usually obtained with binary Ti–Nb alloys [7–9]. Moreover, "flash treatments" (thermal treatment at 700 °C for 3 min for example) carried out on the as-cold rolled Ti2448 alloy allow to further enhance the superelastic property, combined with a very high strength in that case [10]. These properties were recently correlated to the reduced grain size, which is due to the strong applied plastic deformation combined with the following rapid recrystallization treatment in the β phase field [10]. Furthermore, intense plastic deformation is known to induce strong crystallographic texture, which can also influence the mechanical properties and, in the present case, the superelastic behavior of the Ti2448 alloy. As for example, texture evolution after warm rolling was previously investigated in detail in a β titanium alloy [11] and it was evaluated that the superelastic recovery strain is maximized for grains strained along $\langle 1\,1\,0\rangle$ direction [7]. Consequently, a control of the texture can also be used in order to improve the superelasticity of β titanium alloys [7,12].

In this work, moderate, intermediate and high cold rolling reduction rates were used in the Ti2448 alloy in order to vary the crystallographic texture in its solution treated state and after flash thermal treatment. The influence of the resulting texture on the related mechanical properties (tensile strength, Young's modulus, superelastic recovery strain) was investigated in detail.

2. Experiments

A hot-forged Ti2448 cylinder with diameter of 55 mm was used as raw material in this work. The chemical composition of the alloy is given in Table 1. Hot-forged slice-cut samples were directly multi-pass cold rolled without intermediate annealing to reach the final thickness of 0.5 mm. According to different initial thicknesses of the samples used, three reduction rates were obtained: 40% (moderate), 80% (intermediate) and 94% (high). For each reduction rate, two thermal treatments were performed: on the one hand, cold rolled specimens were solution treated under high vacuum at 900 °C for 30 min followed by water quenching (solution treated state, ST); on the other hand, cold rolled specimens were thermally "flash treated" at 700 °C for 3 min followed by air cooling (flash treated state, FT). After thermal treatments, all specimens were cleaned in an acid solution made of 50% HF and 50% HNO_3 (in volume) to remove any oxidation layer. Each specimen is labeled as CR*XX*%-ST and CR*XX*%-FT depending if a solution treatment (ST) or a flash thermal treatment (FT) was performed and where *XX*% mentions the applied cold rolling rate.

Mechanical properties and superelasticity were estimated by conventional and cyclic tensile tests with a strain rate of $10^{-4}\ s^{-1}$. Cyclic tensile tests consist of strain increments of 0.5% followed by stress release up to an elongation of 5%. An extensometer was used to ensure the accuracy of strain. Normalized flat tensile specimens with 3 mm × 15 mm × 0.5 mm gage dimensions were used. The tensile direction was chosen parallel to the rolling direction.

Microstructure was characterized by optical microscopy. Prior to observations, samples were first mechanically polished and next chemically etched with a 15% HNO_3, 8% HF and 77% H_2O solution (vol.%). Transmission electron microscopy (TEM) was also used to characterize the smaller microstructure of FT specimens. Samples were thinned down using a twin-jet electropolishing system with a solution of 4% perchloric acid and 96% methanol (vol.%).

* Corresponding author. Tel.: +33 223238634; fax: +33 223238240.
E-mail address: philippe.castany@insa-rennes.fr (P. Castany).

0925-8388/$ - see front matter © 2013 Elsevier B.V. All rights reserved.
http://dx.doi.org/10.1016/j.jallcom.2013.12.207

Table 1
Chemical composition of hot forged Ti2448 (wt%).

Nb	Zr	Sn	O	Ti
23.9	4.05	8.22	0.16	Bal.

Phase and texture analysis based on X-ray diffraction were conducted on a Philips PW3710 system with Cu Kα1 radiation (λ = 0.154060 nm). For texture analysis, the sample coordinate system was defined as rolling direction (RD), normal direction (ND) and transverse direction (TD). The step size used for the data acquisition is 5°. Orientation Distribution Functions (ODF) were calculated with the raw data of the most important three pole figures (1 1 0), (2 0 0) and (2 1 1) after applying corrections for background and defocusing. Contoured plots of ODF were delineated for constant φ_2 sections in the volume of the reduced Euler space (0° < φ_1, ϕ, φ_2 < 90°).

3. Results and discussion

3.1. Microstructure and phase constitution

The X-ray diffraction patterns of Ti–24Nb–4Zr–8Sn are shown in Fig. 1. Whatever the reduction rate and the thermal treatment applied, only a full-recrystallized β phase microstructure was obtained. Indeed, only (1 1 0), (2 0 0), (2 1 1), and (2 2 0) peaks of the body-centered cubic (bcc) β phase are observed. The lattice parameter of β phase is calculated to be close to 0.3292 nm, which is consistent with the results published previously for the Ti2448 alloy [13]. The microstructure consists of equiaxed grains after solution treatment (Fig. 2a–c) with an average grain size of 60 μm for CR40% and 50 μm for both CR80% and CR94%. After flash thermal treatment, optical micrographs reveal similar microstructures for each cold rolling rate with smaller grains whose size is measured lesser than 10 μm (Fig. 2d–f). However, TEM observations show that the grain size is smaller than what is observed in optical micrographs for the flash thermal treated alloy. The grain size is observed to be independent of the applied cold rolling rate and the microstructures are similar: for example, Fig. 3 illustrates the microstructure with sub-micron grains of the CR94%-FT specimen. For each thermal treatment (ST or FT), the grain size is thus almost independent of the cold rolling rate.

3.2. Mechanical properties

Fig. 4 displays the conventional and cyclic tensile curves obtained after different thermo-mechanical treatments. In Table 2, the mechanical characteristics determined from tensile tests (elongation at rupture, ultimate tensile strength and incipient Young's modulus) are reported.

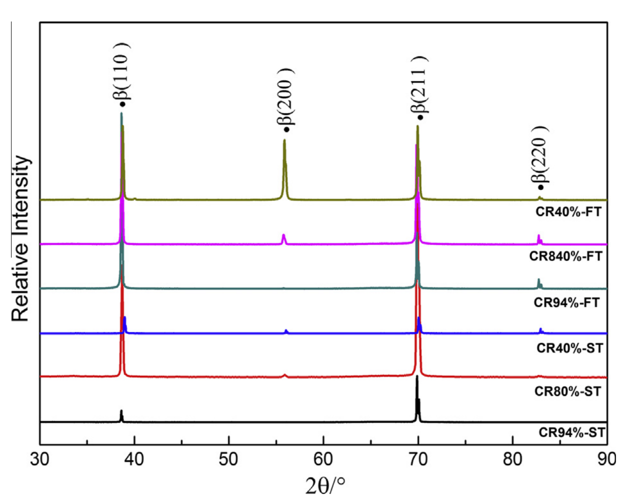

Fig. 1. XRD profiles of Ti2448 alloy after different thermo-mechanical treatments.

Elongation at rupture was evaluated to lie between 8% and 13% and no clear difference in ductility was observed whatever the applied thermo-mechanical process.

From the conventional tensile curves (Fig. 4a and b), a double yielding phenomenon associated to the superelastic property of this alloy is clearly observed, suggesting that α″ martensitic transformation has occurred [7,8]. For both thermal treatments, no clear influence of reduction rate on mechanical properties can be noticed, except for the CR94%-FT sample, where a slight increase of about 50 MPa in ultimate tensile strength can be observed (Fig. 4b and Table 2). However, a strengthening effect can be clearly observed after the flash thermal treatment (Table 2) since higher ultimate tensile strength of about 100 MPa is obtained by comparison to the solution treated alloy. This strengthening effect can be explained by the reduction of the grain size after flash thermal treatment (Figs. 2 and 3), which was also observed in recent works after similar flash thermal treatment [10,14] or warm rolling [1,2,4], in comparison with the large grain size (several tens of micrometers) obtained after solution treatment.

The cyclic stress–strain curves, between 0% and 5% of strain, are given in Fig. 4c and d. All tensile curves display hysteresis loops between loading and unloading, which are due to the reversible stress-induced martensitic transformation. For each cycle, the recovery strain as a function of the applied strain is plotted in Fig. 5 in order to evaluate the evolution of the elastic recovery. As it can be seen on this figure, the most important influential factor is the thermal treatment. Indeed, the highest recovery strain (2.75%) is obtained for the flash treated samples while "only" 2% maximum are reached for the solution treated specimens (at 3.5% of applied strain). It seems also that the maximum recovery strain is enhanced by the increase of cold rolling reduction rate as well, particularly for the solution treated samples.

3.3. Texture evaluation

Fig. 6 shows the different ODF obtained on samples after thermo-mechanical treatments: Fig. 6a–c for the solution treated samples and Fig. 6d–f for the flash thermal treated samples after 40%, 80% and 94% of cold rolling reduction rate, respectively.

After solution treatment, the CR40%-ST sample (Fig. 6a) does not show a strong texture but the main component (0 1 1)[1 0 0] (0°, 45°, 0°) can clearly be identified. For higher reduction rate (CR80%-ST, Fig. 6b), it can be observed preferential orientations on the γ-fiber. The γ-fiber is defined as containing all orientations of (1 1 1) ⟨u v w⟩ type and can be visible on the φ_2 = 45° section where ϕ = 55°. For more precision, the orientation densities are drawn in Fig. 7 with variable φ_1 angle. At intermediate cold rolling rate (Fig. 6b), the texture concentrates mainly on the γ-fiber, that is all the grains are oriented so that a {1 1 1} plane is parallel to the surface of the sample. This γ-fiber is commonly observed in bcc alloys [15–17] and was recently observed in β-titanium alloys after high deformation reduction rates [11]. At high cold rolling rate (CR94%-ST, Fig. 6c) the same observation can be obtained, but the component (1 1 1)[1 $\bar{2}$ 1] appears prominent on this same fiber.

After flash thermal treatment, the lowest cold rolling rate (CR40%-FT, Fig. 6d) exhibits a clear texture corresponding mainly to (2 1 1)[0 $\bar{1}$ 1] (50°, 66°, 63°). With the CR80%-FT sample (Fig. 6e), this orientation remains but orientations along the γ-fiber are also observed as the same shown in the solution treated samples. For the CR94%-FT, only orientations of the γ-fiber are observed (Fig. 6f). It seems that higher the reduction rate is, stronger the γ-fiber is as seen on Fig. 7 wherein the intensity of orientations along this fiber increases with the cold rolling rate. For both thermal treatments, the main component of the γ-fiber is